Supplementary Information: Flash Heating Process for Efficient Meat Preservation

Yimin Mao[1, 2, a], Peihua Ma[3, a], Tangyuan Li[1, a], He Liu[1, a], Xinpeng Zhao[1], Shufeng Liu[1], Xiaoxue Jia[3], Shaik O. Rahaman[3], Xizheng Wang[1], Minhua Zhao[1], Gang Chen[1], Hua Xie[1], Alexandra H. Brozena[1], Bin Zhou[4], Yaguang Luo[4], Rodrigo Tarté[5], Cheng-I Wei[3], Qin Wang[3], Robert M. Briber[1], Liangbing Hu[1, *]

1. Department of Materials Science and Engineering, University of Maryland, College Park, MD, 20742, USA
2. NIST Center for Neutron Research, National Institute of Standards and Technology, Gaithersburg, MD 20899, USA
3. Department of Nutrition and Food Science, University of Maryland, College Park, MD 20742, USA
4. USDA-ARS, Food Quality and Environmental Microbial and Food Safety Laboratories, Beltsville, MD 20705, USA
5. Department of Animal Science, Iowa State University, Ames, IA 50011, USA

Corresponding author: binghu@umd.edu

Table of Contents

Supplementary Figures

Supplementary Table S1. Spectral library search of the liquid chromatography-mass spectroscopy (LC-MS) results of the UFH-treated meat surface

Supplementary Table S2. Spectral library search of the gas chromatography-mass spectroscopy (GC-MS) results of the UFH-treated meat surface

Supplementary Method. High-performance liquid chromatography-mass spectrometry (HPLC-MS) experiment

Supplementary Method. Analysis of the temperature and water content change of beef sample during the UFH treatment

Supplementary Movie S1. The UFH process recorded using a high-speed camera at a collection rate of 200 fps (frame per second)

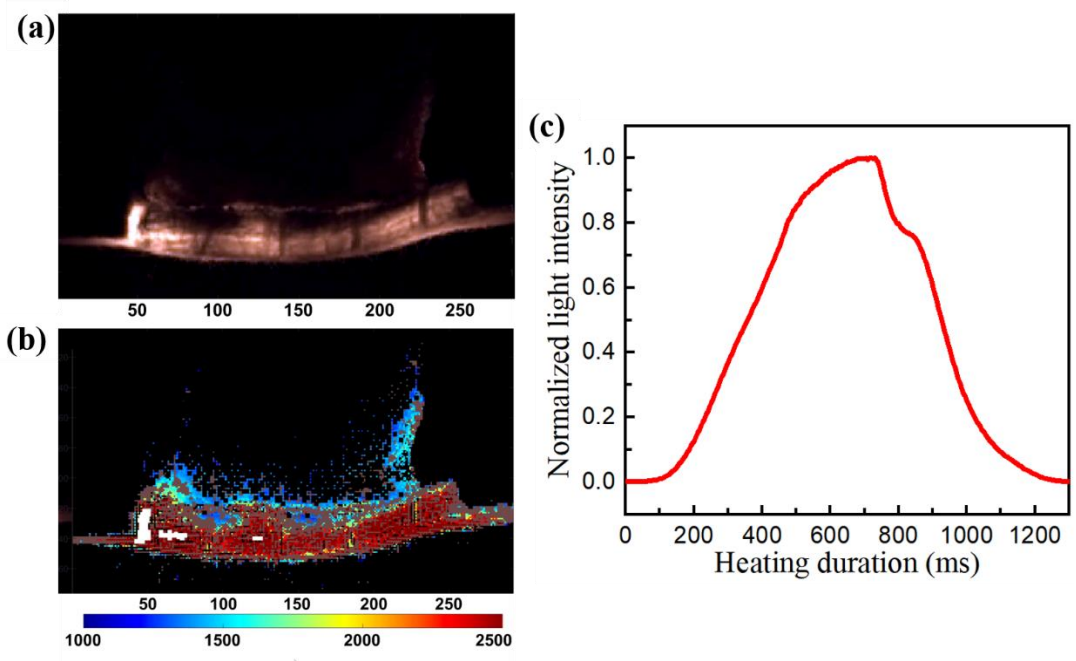

Figure S1: Registering carbon felt light intensity during flashing heating using high speed camera, which is converted to temperature based on previously reported computation protocol. (a) A snapshot of the FH treatment at 700 ms. The bright bottom layer is carbon felt. **(b)** Corresponding temperature distribution across the carbon felt. **(c)** Average light intensity of carbon felt during the FH treatment.

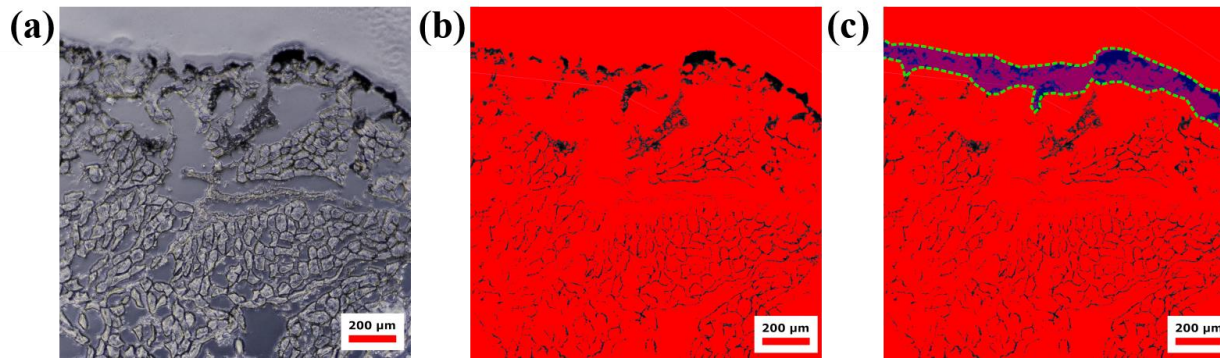

Figure S2: Image analysis of the histological micrographs of UFH-treated beef for the quantification of the surface layer thickness. (a) Original histological micrograph. **(b)** Contrast-enhanced image showing a distinct surface layer. **(c)** Defining the surface layer (blue-shaded region); the layer thickness $d = A/2l$, with A being the area of the shaded region and l the contour length of the boundary (dashed green line). Selection of the surface area region was repeated for 5 times and the average value of layer thickness was reported. The analysis was performed using the imageJ software.

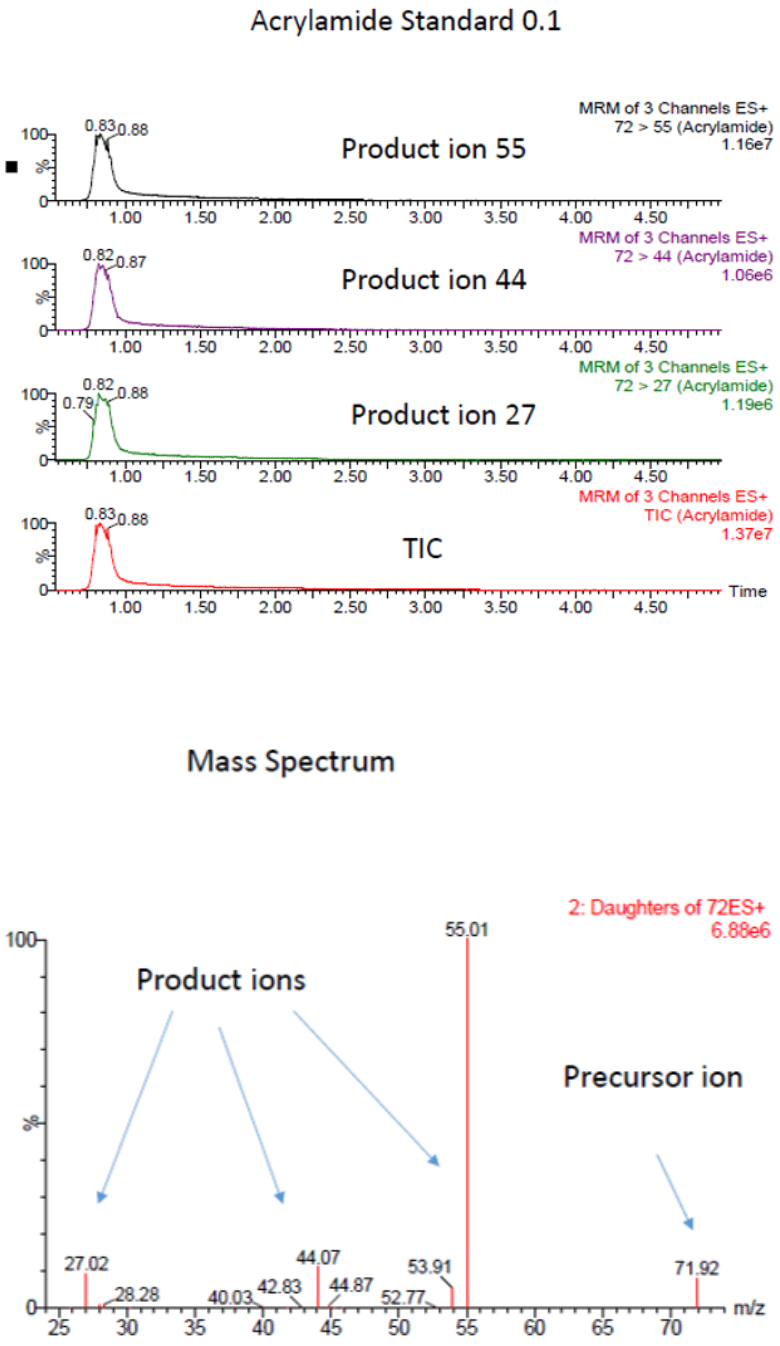

Figure S3: (a)Total ion chromatogram (TIC) overview of acrylamide standard. (b)mass spectrum of acrylamide.

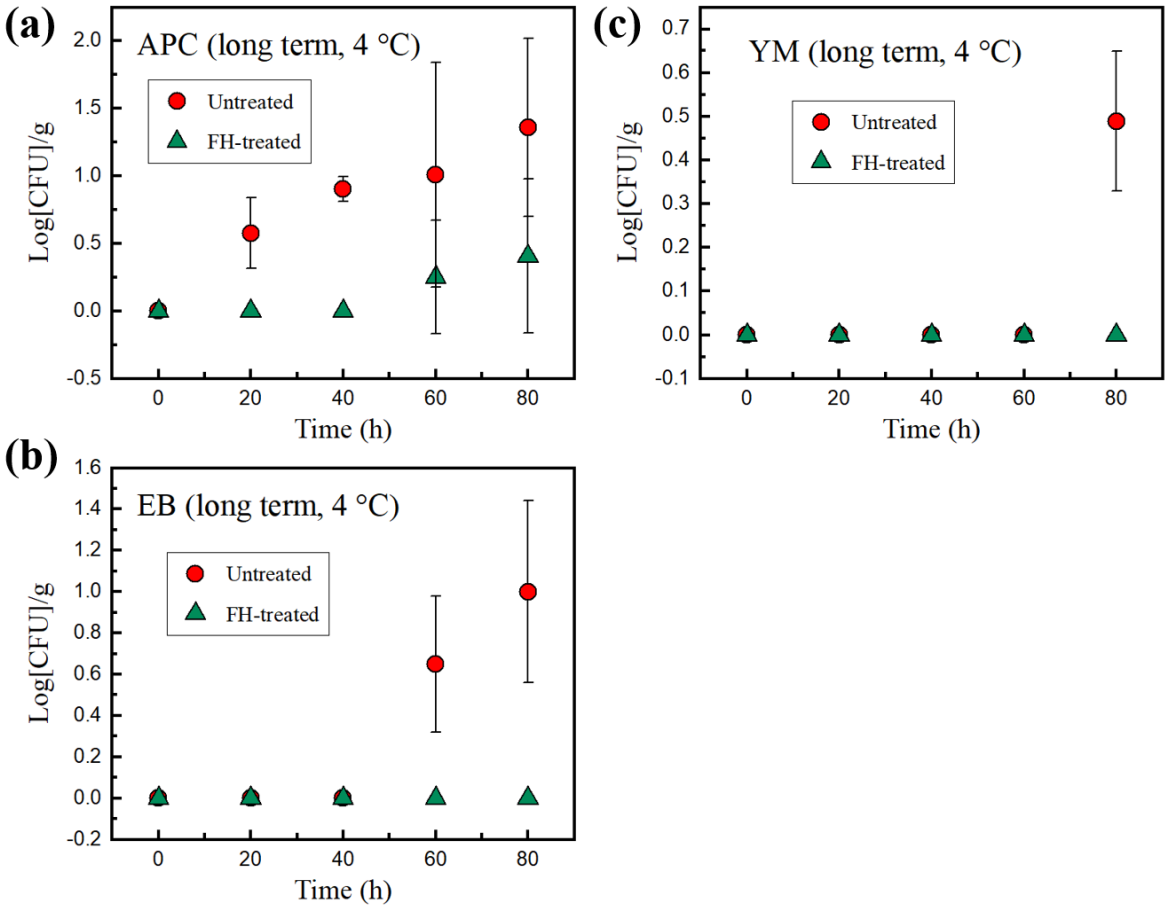

Figure S4: Microbial growth tests of untreated and UFH-treated beef during storage of 80 h at 4 °C. (a) Aerobic plate count (APC). **(b)** Enterobacteriaceae (EB). **(c)** Yeast and mold (YM). Error bars indicates one standard deviation of uncertainty.

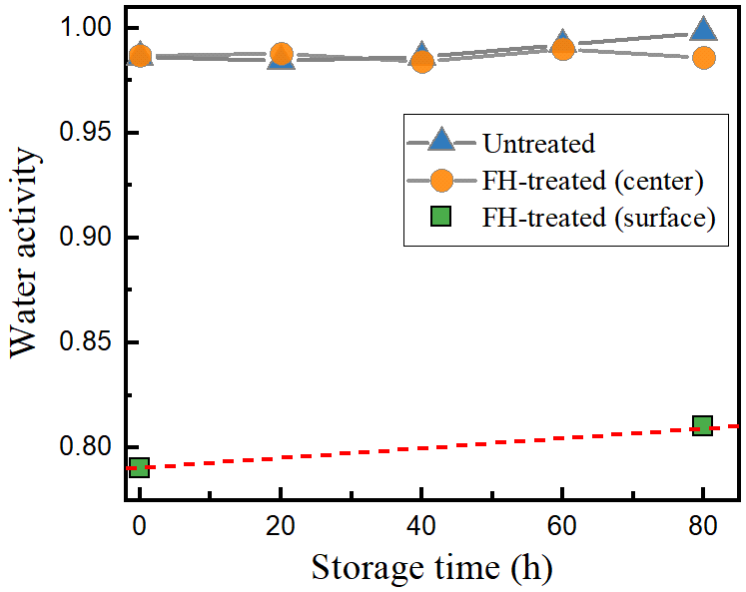

Figure S5: Water activity of untreated and UFH-treated beef during storage. Untreated beef, as well as the center part of the UFH-treated beef, maintain a high level of water activity

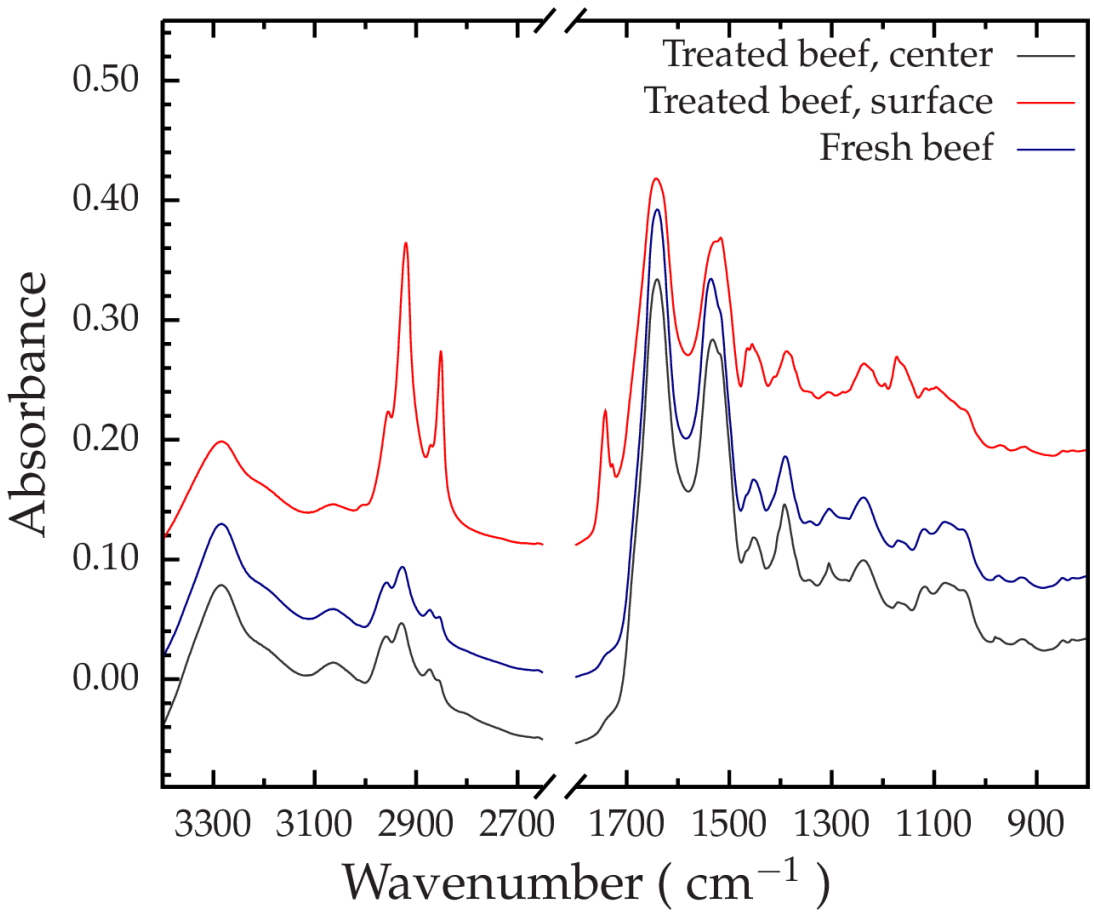

Figure S6: FTIR spectra FH-treated beef (surface and center) and untreated beef.

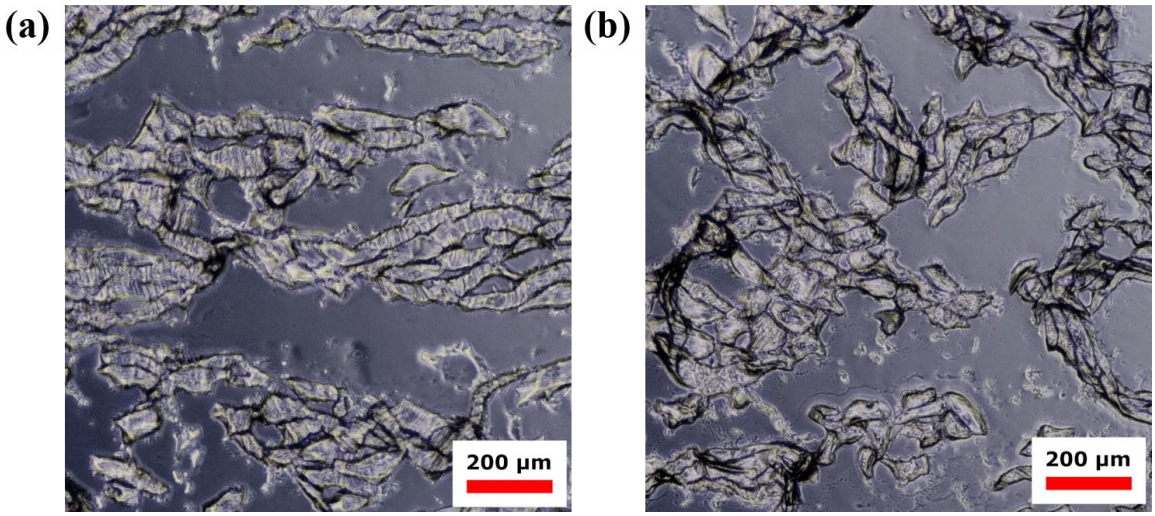

Figure S7: Comparison of histological micrographs of the (a) fresh beef and (b) center part of the UFH-treated beef.

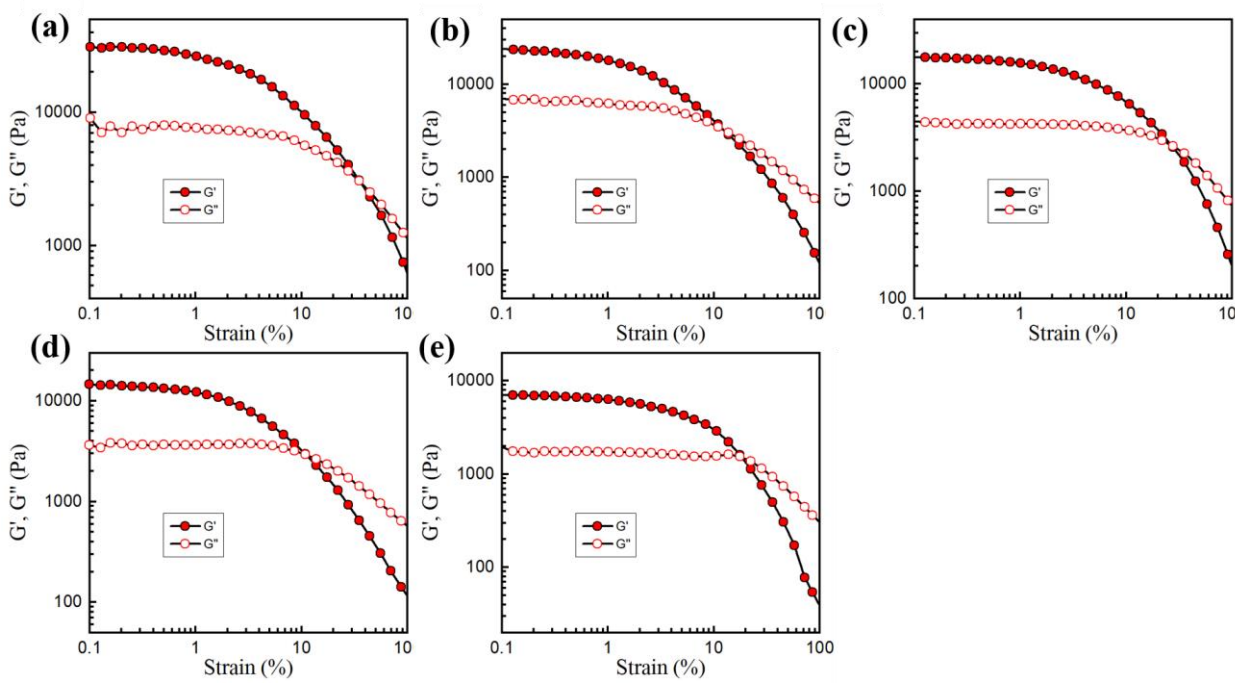

Figure S8: Storage and loss modulus (G' and G") as a function of strain of untreated beef during storage. (a-e) Rheological data at 20, 40, 60, 80, and 100 h.

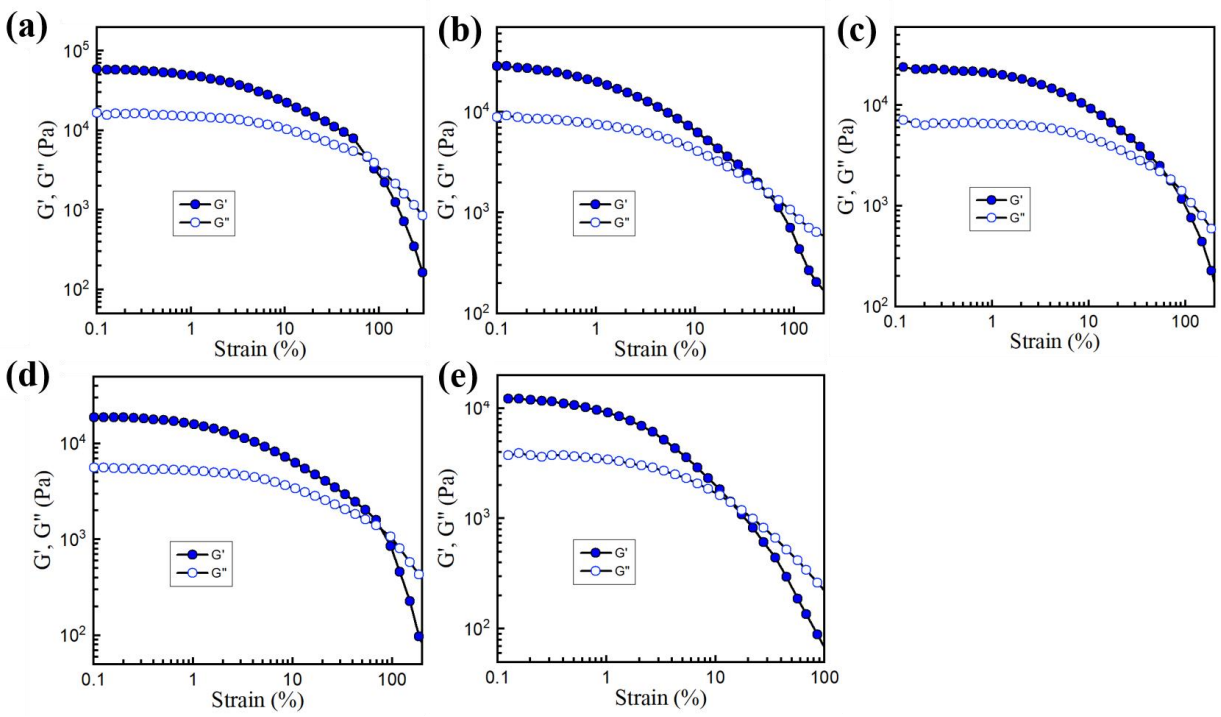

Figure S9: Storage and loss modulus (G' and G") as a function of strain of UFH-treated beef during storage. (a-e) Rheological data at 20, 40, 60, 80, and 100 h.

Table S1. Spectral library search of the LC-MS results of the UFH-treated meat surface

Id	Area	~Retention time (RT)	Compound name	Matches cosine score
253	5.45E+07	0.3865	ACETYL-CARNITINE	0.999
587	5.27E+07	0.5829	ACETYL-CARNITINE	0.999
876	4.52E+06	1.2221	PROPIONYLCARNITINE	0.998
170	5.70E+07	0.375	CARNITINE	0.993
7394	6.15E+05	6.7092	Massbank:LU123902 N-Phenyl-1-naphthylamine|N-phenylnaphthalen-1-amine	0.992
7326	1.80E+06	6.6092	palmitoyl carnitine CollisionEnergy:205060	0.99
1156	5.89E+07	1.659	DL-PHENYLALANINE CollisionEnergy:102040	0.989
763	1.11E+07	0.7968	TYROSINE	0.989
407	4.86E+07	0.421	CARNOSINE	0.986
604	5.81E+06	0.5945	Methionine	0.985
956	3.18E+07	1.5061	INOSINE	0.984
626	2.62E+07	0.6293	HYPOXANTHINE	0.983
5315	4.29E+06	2.942	Massbank:RP025502 Hexanoyl-L-Carnitine|L-Hexanoylcarnitine|(3R)-3-	0.982

			hexanoyloxy-4-	
			(trimethylazaniumyl)butanoate	
7611	5.87E+06	7.1046	PC(0:0/18:1); [M+H]+ C26H53N1O7P1	0.982
7500	1.44E+07	6.9234	PC(0:0/16:0); [M+H]+ C24H51N1O7P1	0.981
7342	9.71E+06	6.6208	PC(18:2/0:0); [M+H]+ C26H51N1O7P1	0.98
7262	9.48E+06	6.4957	PC(18:2/0:0); [M+H]+ C26H51N1O7P1	0.979
7680	1.17E+06	7.2036	PC(0:0/18:1); [M+H]+ C26H53N1O7P1	0.978
7239	1.52E+06	6.472	PE(18:2/0:0); [M+H]+ C23H45N1O7P1	0.978
706	3.07E+06	0.7125	xanthine CollisionEnergy:102040	0.975
7860	2.17E+06	7.6943	PC(0:0/18:0); [M+H]+ C26H55N1O7P1	0.974
7482	1.25E+06	6.8995	PC(20:3/0:0); [M+H]+ C28H53N1O7P1	0.972
7349	2.68E+06	6.6208	PC(0:0/20:4); [M+H]+ C28H51N1O7P1	0.97
7568	3.73E+05	7.0395	PE(22:4/0:0); [M+H]+ C27H49N1O7P1	0.97
5699	2.15E+05	3.1514	MassbankEU:SM817801	0.969
			Cinnamamide|(E)-3-phenylprop-2-enamide	
7586	1.17E+06	7.0808	PE(18:1/0:0); [M+H]+ C23H47N1O7P1	0.969
7533	5.12E+06	6.9588	PC(0:0/18:1); [M+H]+ C26H53N1O7P1	0.968
949	6.87E+06	1.5061	HYPOXANTHINE	0.964
7314	1.90E+06	6.5975	PE(18:2/0:0); [M+H]+ C23H45N1O7P1	0.96
802	3.10E+06	0.9104	3-hydroxybutyrylcarnitine	0.957
7176	1.66E+05	6.2373	PC(16:1/0:0); [M+H]+ C24H49N1O7P1	0.95
7184	4.62E+05	6.2515	PC(20:5/0:0); [M+H]+ C28H49N1O7P1	0.949
8478	2.05E+05	9.1848	cholesta-5,7-dien-3beta-ol	0.948

26	7.96E+05	0.3172	HISTIDINE	0.944
7656	2.86E+05	7.1762	PC(22:4/0:0); [M+H]+ C30H55N1O7P1	0.942
6368	3.46E+05	3.9168	OCTANOYLCARNITINE	0.938
649	4.51E+06	0.6293	INOSINE 5'-MONOPHOSPHATE	0.926
6979	1.67E+05	5.3986	LAUROYLCARNITINE	0.906
8046	8.46E+05	8.1381	16-Hydroxyhexadecanoic acid CollisionEnergy:205060	0.897
7841	9.87E+05	7.6665	PE(18:0/0:0); [M+H]+ C23H49N1O7P1	0.88
6759	1.12E+05	4.7271	DECANOYLCARNITINE	0.866
7472	7.26E+05	6.8726	PE(20:3/0:0); [M+H]+ C25H47N1O7P1	0.838
853	1.25E+06	1.0939	Spectral Match to S-(5'-Adenosyl)-L-homocysteine from NIST14	0.824
846	1.45E+06	1.0812	Spectral Match to Glutathione, oxidized from NIST14	0.823

Table S2. Spectral library search of the GC-MS results of the UFH-treated meat surface

Compound match	~RT	Match
Glycerin	7.4	82.2P
4H-Pyran-4-one,2,3-dihydro-3,5-dihydroxy-6-methyl-	7.96	92.2P
Octanoic acid	8.03	72.5P
2(3H)-Furanone,dihydro-4-hydroxy-	8.14	95.9P
Decanoic acid	9.14	74.7P
Dodecanoic acid	10.19	75.3P

Supplementary Method. High-performance liquid chromatography-mass spectrometry (HPLC-MS) experiment

In our HPLC-MS experiment, we utilized two distinct setups to analyze complex samples. The first setup employed an Orbitrap Q-Exactive mass spectrometer, using a Waters ACQUITY BEH C18 column with a fine particle size of 1.7 μm and a length of 50 mm. This setup was designed for high-resolution and accurate mass measurements, suitable for the analysis of a wide range of analytes in complex mixtures. We used a gradient of water containing 0.1% formic acid (Solvent A) and acetonitrile containing 0.1% formic acid (Solvent B), which was increased from 0% to 95% B over 10 minutes. The second setup involved the Waters Xevo TQ-XS, a triple quadrupole mass spectrometer, which excels in quantitative analysis. This setup used a faster gradient over 5 minutes and an Imtakt Intrada Amino Acid column, specialized for amino acid analysis. Both methods showcase the versatility of HPLC-MS in handling different analytical requirements, from broad-spectrum analysis with the Orbitrap to targeted, sensitive detection with the triple quadrupole.

Supplementary Method. Analysis of the temperature and water content change of the beef sample during the UFH treatment.

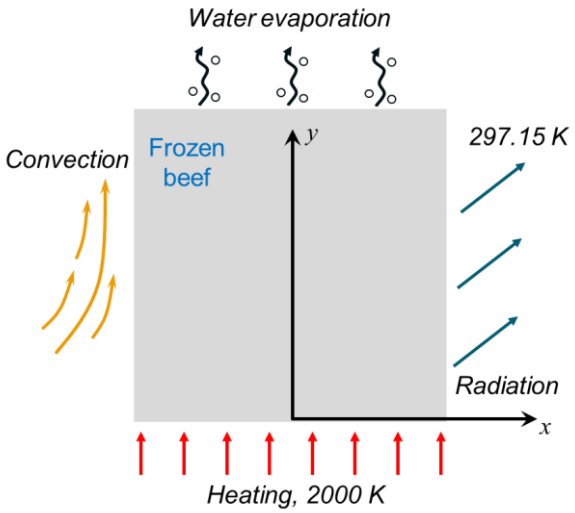

Figure S10: Schematic diagram of heat and water vapor transport during ultra-high temperature exposure of frozen beef at -20 °C.

At the initial time ($t = 0$), a carbon heater, powered by a direct current (DC) supply and located at the bottom of the frozen beef, generates a high temperature of 2000 K lasting for 1 second. This heat is transferred to the frozen beef, potentially increasing its temperature, melting the ice, and causing the water within the beef to evaporate. Concurrently, the beef exchanges heat with its surroundings mainly through convection and radiation. By assuming uniformity in the beef, the variation of the temperature ($T(t,x,y)$) and water content ($C(t,x,y)$) within it can be approximately described as follows:

$$\rho C_p \frac{\partial T(t,x,y)}{\partial t} = k\nabla^2 T(t,x,y) \quad (1)$$

$$\frac{\partial C(t,x,y)}{\partial t} = D\nabla^2 C(t,x,y) \quad (2)$$

where ρ (kg/m^3) is the density of the beef, C_p (J/(kg·K)) denotes the heat capacity of the beef, k indicates the temperature-dependent thermal conductivity[Error! Reference source not found.], and D represents the diffusion coefficient of the water[Error! Reference source not found.]. Here we assume that water mass transfer in the beef does not initiate until the beef is unfrozen, meaning ice sublimation and mass transfer can be neglected before the beef melts ($D = 0\ \mathrm{m}^2/\mathrm{s}$). We employed the apparent heat capacity method to solve the heat transfer equation (Eq. (1)), assuming that beef melting occurs within a specific temperature interval. The latent heat of melting is taken into account by the modification of the specific heat capacity, which is expressed by:

$$c_p = \theta_s c_{p,s} + \theta_l c_{p,l} + L_{s\to l}\frac{\partial \alpha_m}{\partial T} \tag{3}$$

where θ_s and $c_{p,s}$ represent the volume fraction and specific heat capacity of the beef before melting, respectively; θ_l, and $c_{p,l}$ represent the volume fraction and specific heat capacity of the beef before melting. $L_{s\to l}$ is the latent heat of melting, and α_m is defined as the mass fraction of the melted beef. Assuming that water evaporation occurs only on the surface of the beef, the boundary conditions of the heating surface and other surfaces for heat transfer equation (Eq. (1)), including convective, radiative, and evaporative heat transfer, can be described as follows, respectively:

$$k\nabla T = h(T_{air} - T) + \varepsilon\sigma(T_h^4 - T^4) + DL_{l\to g}\nabla C \tag{4}$$

where h (W/(m^2·K)) is the convection heat transfer coefficient, T_{air} (K) and T_h (K) denote the surrounding air temperature and the heater temperature, respectively, $L_{l\to g}$ is defined as the molar latent heat of vaporization, ε refers to the surface emissivity of the beef, σ is the Stefan-Boltzmann

constant, and $DL_{l\to g}\nabla C$ denotes the heat flux out due to moisture vaporization. According to the conservation of mass, the boundary condition for mass transfer equation (Eq. (2)) is as follows:

$$D\nabla C = k_c(C_b - C) \tag{5}$$

where C_b denotes the air moisture concentration and $k_c = h_m/(\rho_{p,l} \cdot C_m)$ is defined as the mass transfer coefficient of the water. In this context, h_m is mass transfer coefficient in mass units and C_m is the specific moisture capacity. In the simulations, the initial temperature (T_0) is set at 253.15 K, and the initial water concentrations of the beef is roughly estimated by $C_0 = \varphi\rho_{p,l}/M_{H_2O}$, where $\varphi = 0.75$ represents the water content. The surrounding air temperature is 293.15 K and the convection heat transfer coefficient is 13.75 W/(m²·K). More details can be found in Table 1.

Table S1. List of the parameters used for simulation.

Parameters	Value	Description
T_{air}	293.15 K	surrounding air temperature
T_0	253.15 K	initial temperature of the beef
h	13.75 W/(m²·K)	convection heat transfer coefficient
M_{H_2O}	0.018 kg/mol	water molecular weight
C_0	43542 mol/m³	initial moisture concentration
C_b	1161.1 mol/m³	air moisture concentration
C_m	0.003	specific moisture capacity
h_m	1.67×10^{-6} kg/(m²·s)	mass transfer coefficient in mass units
k_c	5.33×10^{-7} m/s	mass transfer coefficient
$L_{l\to g}$	41400 J/mol	molar latent heat of evaporation
$L_{s\to l}$	180.8 kJ/kg	latent heat of melting
$\rho_{p,l}$	1045 kg/m³	density of melted beef
$\rho_{p,s}$	961 kg/m³	density of frozen beef
$c_{p,l}$	3510 J/(kg·K)	specific heat capacity of melted beef
$c_{p,s}$	2090 J/(kg·K)	specific heat capacity of frozen beef

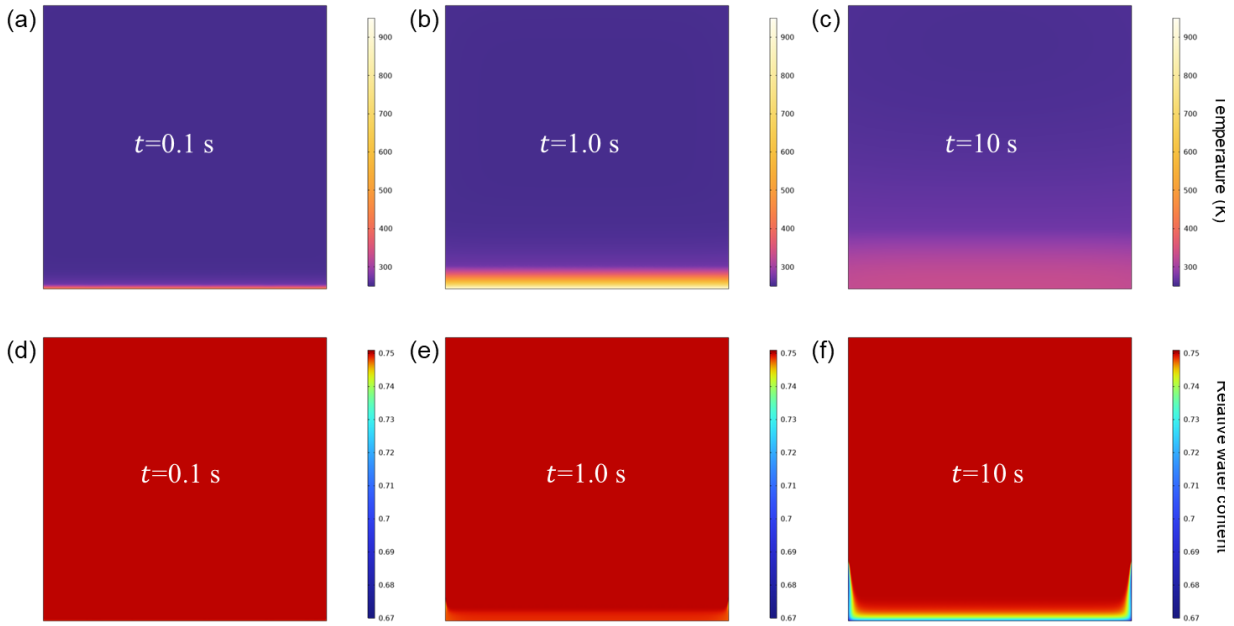

Figure S11: Simulated (a-c) temperature distribution and (d-f) relative water content distribution in the heated beef.

References

1. Willix, J., Lovatt, S. J, Amos, N. D. Additional thermal conductivity values of foods measured by a guarded hot plate. *J. Food Eng.*, 1998, **37(2)**, 159-174.

2. Trujillo, F. J., Wiangkaew C., Pham Q. T. Drying modeling and water diffusivity in beef meat. J. Food Eng., 2007, **78(1)**, 74-85.